# Pressure-Induced Stabilization and Insulator-Superconductor Transition of BH

Chao-Hao Hu,[1,2,*] Artem R. Oganov,[2,3] Qiang Zhu,[2] Guang-Rui Qian,[2] Gilles Frapper,[4] Andriy O. Lyakhov,[2] and Huai-Ying Zhou[1]

[1]*School of Materials Science and Engineering, Guilin University of Electronic Technology, Guilin 541004, People's Republic of China*
[2]*Department of Geosciences, Department of Physics and Astronomy, Stony Brook University, Stony Brook, New York 11794, USA*
[3]*Geology Department, Moscow State University, Moscow 119992, Russia*
[4]*IC2MP UMR 7285, Université de Poitiers - CNRS, Poitiers 86022, France*

(Received 12 January 2013; published 19 April 2013)

Diborane ($B_2H_6$), a high energy density material, was believed to be stable in a wide $P$, $T$ interval. A systematic investigation of the B-H system using the *ab initio* variable-composition evolutionary simulations shows that boron monohydride (BH) is thermodynamically stable and can coexist with solid B, $H_2$, and $B_2H_6$ in a wide pressure range above 50 GPa. $B_2H_6$ becomes unstable and decomposes into the *Ibam* phase of BH and $H_2$ ($C2/c$) at 153 GPa. The semiconducting layered *Ibam* structure of BH at 168 GPa transforms into a metallic phase with space group $P6/mmm$ and a 3D topology with strong B-B and B-H covalent bonds. The *Ibam*-$P6/mmm$ transformation pathway suggests the possibility of obtaining the metastable *Pbcm* phase on cold decompression of the $P6/mmm$ phase. The electron-phonon coupling calculations indicate that $P6/mmm$-BH is a phonon-mediated superconductor with a critical temperature of superconductivity ($T_c$) of 14.1–21.4 K at 175 GPa.

DOI: 10.1103/PhysRevLett.110.165504 PACS numbers: 61.50.Ks, 63.20.D−, 71.20.−b

Pressure can influence the physical and chemical properties of matter, and high-pressure research has uncovered many novel phenomena and greatly changed our fundamental understanding of organic and inorganic materials [1]. One of the most important aspects is pressure-induced superconductivity: numerous experiments have confirmed that many elements and compounds, which are insulators at ambient pressure, can become superconductors under sufficient compression. In particular, hydrogen-rich compounds, such as silane ($SiH_4$) and germane ($GeH_4$), can become high-temperature superconductors at lower pressures than pure hydrogen, owing to ''chemical precompression'' [2]. Recent experimental discoveries [3,4] and theoretical predictions [5,6] have provided evidence for metallization of these hydrogen-dominant compounds. New hope for exploring superconductivity based on metallic hydrogen and possessing unprecedentedly high $T_c$ has been sparked again.

$B_2H_6$, the simplest stable boron hydride at ambient conditions, is a classical electron-deficient molecule and has been extensively used as a highly reactive and versatile reagent [7]. High-pressure experimental and theoretical studies have shown that compressed diborane undergoes a sequence of phase transitions. With increasing pressure to 50 GPa, several structural transitions have been identified in recent spectroscopic experiments [8,9]. However, no detailed experimental structural data are yet available for these high-pressure phases. More recently, theoretical calculations within density functional theory (DFT) have indicated that molecular diborane first transforms into a molecular crystal made of discrete $BH_3$ trimers near 4 GPa, and a polymeric crystal containing one-dimensional chains becomes more stable above 36 GPa [10]. However, another detailed DFT investigation [11] shows that $B_2H_6$ becomes unstable in the pressure range of 40–350 GPa and decomposes into B and $H_2$. The discrepancy between these investigations encourages us to further investigate the high-pressure behavior of $B_2H_6$ in detail in the present work.

To find stable and low-enthalpy metastable structures, we used the evolutionary algorithm USPEX, implemented in the USPEX code [12–14], which has been widely used to predict stable high-pressure crystal structures without requiring any experimental information [6,15–17]. In particular, we used not only the traditional fixed-composition searches [12,13], but also the newly developed variable-composition technique [18,19], also available in the USPEX code. This powerful technique enables one to find, in a single simulation, all stable compounds and their crystal structures in a multicomponent system (in this case, the B-H system). Evolutionary crystal structure prediction calculations were performed at 10, 20, 50, 100, 200, and 300 GPa. The underlying structural relaxations and electronic structure calculations presented here were performed using the all electron projector augmented wave method [20] as implemented in the Vienna *ab initio* simulation package (VASP) [21]. The exchange-correlation energy was treated within the generalized gradient approximation, using the functional of Perdew, Burke, and Ernzerhof [22]. A plane-wave cutoff energy of 540 eV and dense Monkhorst-Pack $k$-point meshes [23] with the reciprocal space resolution of $2\pi \times 0.03$ Å$^{-1}$ were used for all structures to ensure that the enthalpy calculations are converged to better than 1 meV/atom.

 

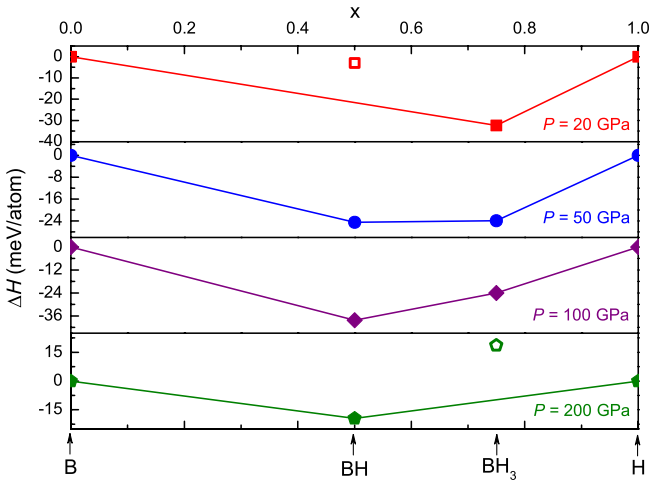


FIG. 1 (color online). Enthalpies of formation ($\Delta H$, in meV/atom) with respect to B and H for the B-H systems at 20, 50, 100, and 200 GPa.

Structural transition pathways were explored with the variable-cell nudged elastic band (VC-NEB) method [24], implemented in USPEX. The convergence criteria for the root-mean-square force were 0.03 eV/Å for each image. Lattice dynamics and electron-phonon coupling (EPC) calculations for the $P6/mmm$ structure of BH were performed with the QUANTUM-ESPRESSO package [25] using ultrasoft pseudopotentials and plane wave basis sets with a kinetic energy cutoff of 180 Ry. A $24 \times 24 \times 16$ Monkhorst-Pack $k$-point grid with a Gaussian smearing of 0.05 Ry was used for self-consistent calculations, which ensures that EPC matrix elements are sufficiently accurate. A $6 \times 6 \times 4$ $q$-point mesh in the first Brillouin zone was used for the calculation of EPC matrix elements.

Figure 1 shows the enthalpy of formation ($\Delta H$) for B-H compounds at selected pressures. Interestingly, besides reproducing various structures of solid $B_2H_6$ [10,11], B [15], and $H_2$ [26], previously unreported boron monohydride (BH) is found to be stable in a wide pressure range in our evolutionary structure search. It can be found from Fig. 1 that at around 20 GPa the orthorhombic BH with space group $Pbcm$ is still metastable and lies above the tie line joining $\gamma$-$B_{28}$ [15] and the $P$-1 structure of $B_2H_6$ [10]. At 50 and 100 GPa, we predict stable phases of B ($\gamma$-$B_{28}$ and $\alpha$-Ga-type), BH ($Ibam$), $B_2H_6$ ($P2_1/c$), and $H_2$ ($P6_3/m$). At 200 GPa, $B_2H_6$ is already unstable and decomposes into BH ($P6/mmm$) and $H_2$ ($C2/c$). More detailed convex hull diagrams for the B-H system at different pressures can be found in the Supplemental Material [27].

Pressure-composition high-pressure phase diagram of the B-H system is depicted in Fig. 2(a) and shows the stability ranges of solid B, BH, $B_2H_6$, and $H_2$. It can be seen that $B_2H_6$ (space group $P2_1/c$) becomes unstable and decomposes into BH ($Ibam$) and $H_2$ ($C2/c$) at 153 GPa, and the $P6/mmm$ structure of BH becomes more stable than the $Ibam$ structure at 168 GPa. Two out of three

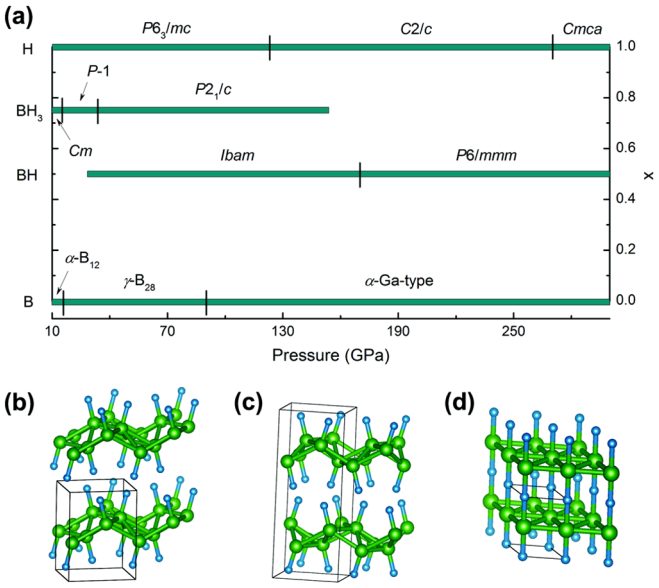


FIG. 2 (color online). Phase stability in the B-H system: (a) Schematic representation of the phase diagram in the pressure range from 10 to 300 GPa and structures of BH phases with space groups (b) $Pbcm$ at 20 GPa, (c) $Ibam$ at 150 GPa, and (d) $P6/mmm$ at 175 GPa. Large green and small blue spheres are B and H, respectively.

competitive BH phases, shown in Figs. 2(b)–2(d), have layered structures. The 2D structures of the $Pbcm$ and $Ibam$ phases of BH consist of the same puckered BH layers arranged in different orientations; in each layer, every B atom has six boron neighbors in the puckered close-packed boron layer, and one hydrogen atom above or below the layer. 3D topology is present in the $P6/mmm$ phase—here, we have flat close-packed boron layers, with H atoms located symmetrically between the B layers and connecting to them by strong B-H bonds. Figures 2(b)–2(d) shows the structural changes that occur in BH under pressure.

Using the VC-NEB method, we have simulated the transition pathway between thermodynamically stable $Ibam$ and $P6/mmm$ phases. The results (Fig. 3) reveal that the $Ibam \rightarrow P6/mmm$ reconstructive phase transition can be considered as a two-stage transformation. First, the $Ibam$ structure of BH transforms to the metastable $Pbcm$ structure (this transition has a high barrier, 0.32 eV/f.u. at 168 GPa), with BH layers changing from an antiparallel to parallel arrangement making it easier for interlayer bonds to form. In the second stage, the puckered BH layers gradually flatten, with H atoms gradually occupying positions exactly between two boron layers and forming strong B-H bonds (one with each layer). This stage encounters a much lower energy barrier (0.19 eV/f.u.). This picture implies that the $Pbcm$ structure of BH may be synthesized in experiment as a metastable product of cold decompression of the $P6/mmm$ phase.

The zero-point energy (ZPE) may play an important role in determining the relative stability of hydrogen-rich

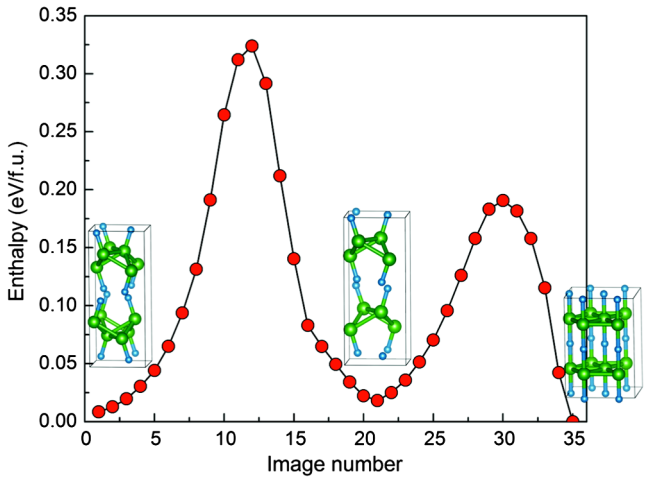


FIG. 3 (color online). Calculated transformation barrier for the $Ibam \rightarrow P6/mmm$ transition of BH at 168 GPa from the VC-NEB method. The intermediate *Pbcm* phase is detected at the image 21 along the pathway.

phases [6,26]. However, our calculations results show that ZPE does not change the topology of high-pressure phase diagram of BH [27] and quantitative effects are modest. For example, the ZPE differences (11.5 ~ 32.7 meV/f.u. in the 100–200 GPa pressure range) between the *Pbcm*, *Ibam*, and $P6/mmm$ structures of BH shift the $Ibam \rightarrow P6/mmm$ transition pressure from 168 to 159 GPa. A detailed comparison of the relative stability of $B_2H_6$, $B + H_2$, and $BH + H_2$ shows that $BH + H_2$ is more stable than $B + H_2$ in the pressure range 20–300 GPa [27]. The destabilization of $B_2H_6$ can be traced to the well-known tendency for electronic delocalization under pressure—here, it is manifested in the formation of a larger number of relatively weak multicenter B-B bonds, satisfying a larger share of valence needs of boron atoms and liberating hydrogen atoms. This tendency has two consequences: (1) the enthalpies of formation of B-H compounds from B and $H_2$ become quite small under pressure (~15 meV/atom for BH at 200 GPa), (2) a greater number of B-B bonds and a greater degree of electronic delocalization eventually lead to metallization. While the *Pbcm* and *Ibam* phases are semiconducting, the $P6/mmm$ phase is a metal.

Figure 4 shows the electronic band structure and projected density of states (DOS) of B-2$p_{x,y}$, B-2$p_z$, and H-1*s* for the $P6/mmm$ structure of BH at 175 GPa. The DOS of B-2*s* is not presented here, since its contribution to the total DOS in the vicinity of Fermi level ($E_F$) is very small. Two bands, marked as "band1" and "band2" in Fig. 4(a), cross the $E_F$ and have widths of 17.9 and 25.9 eV, respectively,

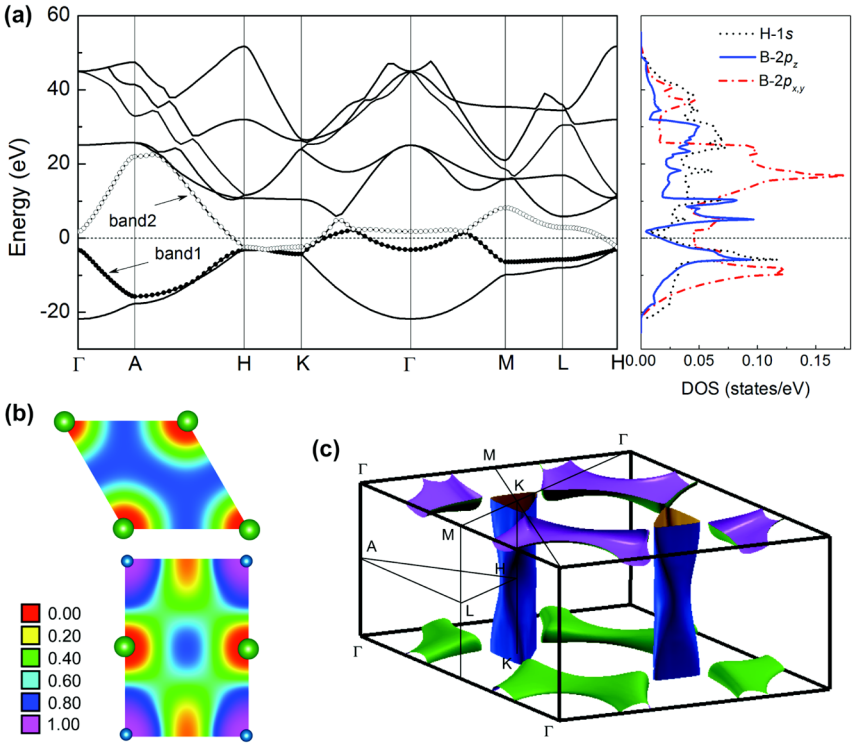


FIG. 4 (color online). Electronic structure of the $P6/mmm$ phase of BH at 175 GPa. (a) Band structure along the selected high-symmetry lines and atom-projected DOS, where the dotted lines at zero indicate the Fermi level. (b) ELF for the (0001) plane passing through B atoms and the (1010) plane through B and H atoms. (c) Holelike FS with purple (or green) fragments of hexagonal toroidal pockets originating from the hybridized H-1*s* and B-2$p_z$ bonding $\sigma$ band and electronlike FS with blue cylinders from the B-2$p_{x,y}$ bonding $\sigma$ band, which corresponds to the band1 and band2 that cross the Fermi level as marked in (a).

which play a crucial role in determining the superconducting behavior of the metallic $P6/mmm$ phase. As shown in Fig. 4(a), band1 makes two small hole pockets along the $K$-Γ-$M$ path, which is mainly composed of hybridized B-$2p_z$ and H-1$s$ states, while electron pockets around the $H$ and $K$ points in band2 are made of B-$2p_{x,y}$ states. The total DOS at $E_F$, $N(E_F)$, is 0.11 states/eV/f.u. for the $P6/mmm$ structure at 175 GPa, where the contributions from B and H are about 57% and 20%, respectively. The calculated electron localization function (ELF) shown in Fig. 4(b) is helpful for clearly understanding the bonding nature of the $P6/mmm$ structure. The maximum ELF value for the B-B bonds is 0.76, indicating delocalized covalent bonding in the boron sheets, while the ELF value close to 1.0 between B and H suggests strong polar covalent bonding. The Fermi surface (FS) of the $P6/mmm$ phase shown in Fig. 4(c) consists of two sheets owing to the two bands (band1 and band2) crossing the $E_F$. The FS sheet from band1 located at the $k_z = 0$ plane is a toroidal pocket with a 2D shape and hole character. The cylinderlike FS sheet from band2 is electronlike, centered along the $K$-$H$ line and parallel to the $k_z$ direction.

The calculated phonon dispersion curves and projected phonon DOS for the $P6/mmm$ structure of BH at 175 GPa are presented in Fig. 5. The absence of any imaginary frequencies indicates dynamical stability. The low-frequency bands below 1040 $cm^{-1}$ come mainly from the strongly coupled vibrations between B and H, while higher-frequency modes (in the ranges 1040–1682 and 2403–2864 $cm^{-1}$) are mostly related to the H atoms. To explore the possible superconductivity of BH, electron-phonon coupling (EPC) calculations for the $P6/mmm$ structure at 175 GPa were performed. The corresponding

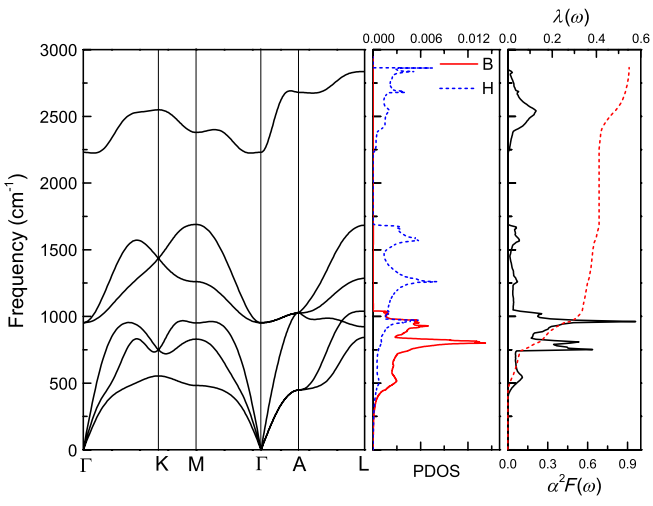


FIG. 5 (color online). Phonon dispersion curves, phonon density of states (PDOS) projected on B and H atoms, and Eliashberg phonon spectral function $\alpha^2F(\omega)$ together with the electron-phonon integral $\lambda(\omega)$ for the $P6/mmm$ structure of BH at 175 GPa.

Eliashberg spectral function $\alpha^2F(\omega)$ and the EPC parameter $\lambda$ as a function of frequency are shown in Fig. 5. The resulting integral $\lambda$ is 0.55, indicating a strong EPC in the $P6/mmm$ structure. Coupled B-H vibrations in the frequency region below 1040 $cm^{-1}$ contribute about 61.6% of the total $\lambda$, while H vibrations in the regions from 1040 to 1682 $cm^{-1}$ and above 2403 $cm^{-1}$ contribute 13.6% and 24.8% of $\lambda$, respectively. Using the calculated logarithmic average frequency $\omega_{\log}$ (1261.8 K) and commonly accepted values of the Coulomb pseudopotential $\mu*$ (0.1 and 0.13), from the Allen-Dynes modified McMillan equation [28] we obtain the critical temperature of superconductivity ($T_c$) in the range 14.1–21.4 K at 175 GPa. The pressure dependence of $\lambda$, $\omega_{\log}$, and $T_c$ for the $P6/mmm$ structure is given in Supplemental Materials [27]. The calculated $T_c$ decreases monotonically with pressure at an approximate rate of −0.21 K/GPa (30.8–39.2 K at 100 GPa and 11.7–18.8 K at 200 GPa). There are similarities in the structures and superconducting behavior of the $P6/mmm$ structure of BH and the extensively studied $P6/mmm$ $MgB_2$ [29–31]. However, superconductivity in $MgB_2$ is exclusively due to the B sheets, while in BH it is due to both B and H sublattices.

In summary, the energetically favorable high-pressure phases of the solid B-H system have been investigated in detail using *ab initio* evolutionary structure prediction. Our results indicate that BH, reported for the first time in the present work, is a thermodynamically stable compound that can coexist stably with solid B, $H_2$, and $B_2H_6$ in a wide pressure range from 50 to 153 GPa, and above 153 GPa is the only stable boron hydride. At 168 GPa, BH undergoes a phase transition from the semiconducting *Ibam* phase to the metallic $P6/mmm$ phase. The predicted phase transition mechanism involves an intermediate metastable *Pbcm* phase, which may be synthesized by cold decompression of the $P6/mmm$ phase. Electron-phonon coupling calculations show that the $P6/mmm$ phase of BH is a phonon-mediated superconductor with a $T_c$ of 14.1–21.4 K at 175 GPa, its $T_c$ decreases with pressure at an approximate rate of −0.21 K/GPa, which is comparable to that of $MgB_2$. However, unlike in $MgB_2$, superconductivity of the $P6/mmm$ BH arises not only from the close-packed B layer, but also from the H atoms.

This work was supported by the National Natural Science Foundation of China under 50901023 and 11164005 and the Guangxi Natural Science Foundation under 2010GXNSFD013009 and 2012GXNSFGA060002. A. R. O. acknowledges funding from DARPA (Grants No. N660011014037 and No. W31P4Q1210008) and NSF (Grant No. EAR-1114313). The calculations were performed at the supercomputer of the Center for Functional Nanomaterials, Brookhaven National Laboratory, which is supported by the U.S. Department of Energy, Office of Basic Energy Sciences, under Contract No. DE-AC02-98CH10086.

*To whom all correspondence should be addressed.
chaohao.hu@guet.edu.cn

[1] R. J. Hemley and N. W. Ashcroft, Phys. Today **51**, 26 (1998).
[2] N. W. Ashcroft, Phys. Rev. Lett. **92**, 187002 (2004).
[3] X. J. Chen, V. V. Struzhkin, Y. Song, A. F. Goncharov, M. Ahart, Z. Liu, H. Mao, and R. J. Hemley, Proc. Natl. Acad. Sci. U.S.A. **105**, 20 (2008).
[4] M. I. Eremets, I. A. Trojan, S. A. Medvedev, J. S. Tse, and Y. Yao, Science **319**, 1506 (2008).
[5] J. Feng, W. Grochala, T. Jaroń, R. Hoffmann, A. Bergara, and N. W. Ashcroft, Phys. Rev. Lett. **96**, 017006 (2006).
[6] M. Martinez-Canales, A. R. Oganov, Y. Ma, Y. Yan, A. O. Lyakhov, and A. Bergara, Phys. Rev. Lett. **102**, 087005 (2009).
[7] B. M. Mikhailov, Russ. Chem. Rev. **31**, 207 (1962).
[8] Y. Song, C. Murili, and Z. Liu, J. Chem. Phys. **131**, 174506 (2009).
[9] C. Murili and Y. Song, J. Phys. Chem. B **113**, 13 509 (2009).
[10] Y. Yao and R. Hoffmann, J. Am. Chem. Soc. **133**, 21 002 (2011).
[11] K. Abe and N. W. Ashcroft, Phys. Rev. B **84**, 104118 (2011).
[12] A. R. Oganov and C. W. Glass, J. Chem. Phys. **124**, 244704 (2006).
[13] A. R. Oganov, A. O. Lyakhov, and M. Valle, Acc. Chem. Res. **44**, 227 (2011).
[14] A. O. Lyakhov, A. R. Oganov, H. T. Stokes, and Q. Zhu, Comput. Phys. Commun. **184**, 1172 (2013).
[15] A. R. Oganov, J. Chen, C. Gatti, Y. Ma, Y. Ma, C. W. Glass, Z. Liu, T. Yu, O. O. Kurakevych, and V. L. Solozhenko, Nature (London) **457**, 863 (2009).
[16] E. Zurek, R. Hoffmann, N. W. Ashcroft, A. R. Oganov, and A. O. Lyakhov, Proc. Natl. Acad. Sci. U.S.A. **106**, 17 640 (2009).
[17] X. D. Wen, L. Hand, V. Labet, T. Yang, R. Hoffmann, N. W. Ashcroft, A. R. Oganov, and A. O. Lyakhov, Proc. Natl. Acad. Sci. U.S.A. **108**, 6833 (2011).
[18] A. R. Oganov, Y. Ma, A. O. Lyakhov, M. Valle, and C. Gatti, Rev. Mineral. Geochem. **71**, 271 (2010).
[19] A. R. Oganov, *Modern Methods of Crystal Structure Prediction* (Wiley-VCH, Weinheim, 2010).
[20] P. E. Blöchl, Phys. Rev. B **50**, 17 953 (1994).
[21] G. Kresse and J. Furthmüller, Phys. Rev. B **54**, 11 169 (1996).
[22] J. P. Perdew, K. Burke, and M. Ernzerhof, Phys. Rev. Lett. **77**, 3865 (1996).
[23] H. J. Monkhorst and J. D. Pack, Phys. Rev. B **13**, 5188 (1976).
[24] G. R. Qian, X. Dong, X. F. Zhou, Y. Tian, A. R. Oganov, and H. T. Wang (to be published).
[25] P. Giannozzi *et al.*, J. Phys. Condens. Matter **21**, 395502 (2009).
[26] C. J. Pickard and R. J. Needs, Nat. Phys. **3**, 473 (2007).
[27] See Supplemental Material at http://link.aps.org/supplemental/10.1103/PhysRevLett.110.165504 for detailed crystal structure information, high-pressure behavior, and electronic properties of B-H compounds.
[28] P. B. Allen and R. C. Dynes, Phys. Rev. B **12**, 905 (1975).
[29] J. Nagamatsu, N. Nakagawa, T. Muranaka, Y. Zenitani, and J. Akimitsu, Nature (London) **410**, 63 (2001).
[30] M. Monteverde, M. Núñez-Regueiro, N. Rogado, K. A. Regan, M. A. Hayward, T. He, S. M. Loureiro, and R. J. Cava, Science **292**, 75 (2001).
[31] J. Kortus, I. I. Mazin, K. D. Belashchenko, V. P. Antropov, and L. L. Boyer, Phys. Rev. Lett. **86**, 4656 (2001).